Adjusting the electrode surface functionality to improve the cell voltage of aqueous electrolyte carbon/carbon supercapacitors

Alicia Gomis Berenguer, Martin Weissmann, Rachelle Omnee, Encarnación Raymundo-Piñero

Carbon 234 (2025) 119927

Contents lists available at ScienceDirect

Carbon

journal homepage: www.elsevier.com/locate/carbon

Adjusting the electrode surface functionality to improve the cell voltage of aqueous electrolyte carbon/carbon supercapacitors

Alicia Gomis Berenguer [a,**], Martin Weissmann [b,c], Rachelle Omnee [b,c], Encarnación Raymundo-Piñero [b,c,*]

[a] Institute of Electrochemistry, University of Alicante, 03080, Alicante, Spain
[b] CNRS, CEMHTI UPR 3079, Univ. Orléans, F - 45071, Orléans, France
[c] Réseau sur le Stockage Electrochimique de l'Energie (RS2E), FR CNRS, 3459, France

ARTICLE INFO

Keywords:
Carbon/carbon supercapacitors
Aqueous electrolyte
Carbon/electrolyte interface
Surface functionality
Asymmetric configuration
Positive electrode protection

ABSTRACT

Improving the performance of supercapacitors in terms of energy density is a major technical challenge, especially in aqueous media where the operating voltage is limited by the electrochemical stability window of water and by undesirable reactions at the electrode/electrolyte interface. Carbon/carbon supercapacitors using 1.0 mol L^{-1} Li_2SO_4 as electrolyte can achieve cell voltages of 1.8 V. Beyond this value, long-term supercapacitor operation is limited by positive electrode degradation due to irreversible oxidation reactions at the carbon/electrolyte interface. Such degradation processes can be minimized by selectively modifying the surface functionality of the porous carbon active electrode material. An in-depth study of the effect of different surface functionalities on the ageing of the supercapacitor, combining quantitative analysis of the gas generated during operation with electrochemical techniques and physical characterization of the carbon electrode, showed that among the different processes, the chemical grafting of low amounts of phenyl functionalities is the most effective in preventing the oxidation of the carbon. The origin of the resistance to oxidation was a combined effect of the blocking of active sites and the reduction of the local pH at the interface. The cell voltage can be increased to 2.2 V and the energy density more than doubled by using an asymmetric system with the modified carbon as the positive electrode and an unmodified carbon as the negative electrode.

1. Introduction

Today, the growing interest in supercapacitors as energy storage devices is driven by the demand for power applications. Supercapacitors are particularly valued for such applications due to their high charge/discharge rates and long-term cycling capabilities. Current industrial technologies for supercapacitors are based on porous carbon electrodes immersed in an organic electrolyte. These organic electrolytes allow operating voltages of 2.8–3.0 V, while equivalent systems in acidic or alkaline aqueous electrolytes, such as H_2SO_4 or KOH, cannot exceed 0.8–1.0 V. However, it has been demonstrated that neutral aqueous electrolytes can be a reliable alternative to organic electrolytes for symmetric carbon/carbon supercapacitors due to their higher operating voltage and more favorable safety and environmental characteristics [1–3]. In the particular case of sulfate-based electrolytes, some reports indicate 2.0–2.2V as the cell voltage, although these conclusions are often based on low-reliability galvanostatic charge-discharge cycling at high current densities. However, by using voltage floating, the stability voltage was revealed more likely to be 1.6–1.8 V, which is still higher than in acidic or basic electrolytes [4,5].

The high operating voltage of carbon/carbon supercapacitors operating in neutral sulfate electrolytes could be attributed to the fact that considering the low OH^- and H^+ concentration in such electrolytes, the local pH at the electrode/electrolyte interface becomes easily acidic or alkaline due to the oxygen evolution reaction (OER) or hydrogen evolution reaction (HER), respectively [6–12]. As a result, the potential for the two reactions is shifted and the total potential window can be expanded. In fact, under negative polarization, the local pH increase of the electrolyte is significantly influenced by the adsorption of nascent hydrogen generated by water splitting at the carbon-electrolyte interface giving rise to a H_2 evolution overpotential [7,13]. Such an effect has been shown to be more pronounced in neutral sulfate-based electrolytes

* Corresponding author. CNRS, CEMHTI UPR 3079, Univ. Orléans, F - 45071, Orléans, France.
** Corresponding author.
E-mail addresses: alicia.gomis@ua.es (A.G. Berenguer), raymundo@cnrs-orleans.fr (E. Raymundo-Piñero).

https://doi.org/10.1016/j.carbon.2024.119927
Received 17 September 2024; Received in revised form 10 December 2024; Accepted 16 December 2024
Available online 18 December 2024

than in acidic or alkaline electrolytes [1,2,4,6]. Therefore, in the particular case of neutral electrolytes, the negative electrode does not limit the operation voltage. However, the maximum operating voltage in an aqueous medium is highly dependent on the positive electrode degradation during cycling [4,5]. For carbon based electrodes under positive polarization, electro-oxidation arises before reaching the thermodynamical limit for water oxidation. Such oxidation induces structural defects on the graphene layers that define the porous network of carbon resulting in collapsing pores and therefore in losing the ability to electroadsorb ions to form the electrical double layer [4]. Therefore, to increase the cell voltage in an aqueous electrolyte, it is necessary to find strategies to protect the positive electrode from oxidation.

The reactivity of a carbon material in an electrolyte will be related to its texture/structure as it depends on the edges of the graphene layers. At these edges, the surface functionalities can modify the electron donor/acceptor character of the graphene layers and affect the charging of the electrical double layer. In addition, highly reactive free edge sites are present together with unpaired electrons stabilized by resonance [14,15]. In the case of carbon-based supercapacitors in organic electrolytes, some reports show that their reactivity is thought to be responsible for electrolyte decomposition and poor cyclability [16], since others relate the corrosion of the positive electrode to H-terminated edge sites and oxygen-functional groups which are decomposed as CO during a thermal treatment [17]. Since carbon materials with a larger number of edge sites would be expected to have a larger number of surface functionalities and unpaired electrons and thus exhibit higher reactivity [15,18], one solution that has been shown in such electrolytes is to use carbon materials with a small number of carbon edge sites, such as graphene mesosponges [19] or high graphitisation degree carbos [20]. However, such an approach would require high-temperature processes resulting in low specific surface areas, which are not plausible for SC applications, or the synthesis of model materials that are not transferable to the industrial scale.

The effect of the surface functionality of carbon-based electrodes in aqueous electrolytes has usually been reported from the point of view of introducing a pseudo-capacitive contribution to be added to the electrical double layer capacitance, but very rarely from the point of view of decreasing the carbon reactivity [21]. In fact, carbon materials doped with heteroatoms can exhibit nobility or resistance to oxidation [22]. In the particular case of neutral electrolytes, the importance of surface functionality for stability was introduced by Gao et al. [2], demonstrating that the carbon electrode can be stabilized to some extent by controlled oxidation with H_2O_2. This hypothesis was later adapted with the electrooxidation of an activated carbon cloth [23]. Moreover, electrooxidation resistance has been shown in such electrolytes by incorporating P-based functional groups [24] or N-doped ones [25,26]. Another approach found in the literature is the use of redox additives such as metallacarboranes, which act as electron consuming agents to prevent carbon oxidation [27].

In this study, several approaches will be explored to modify the surface functionality of the carbon electrode with the intent of reducing the reactivity of the carbon to increase the potential oxidation limit. Traditional chemical oxidation and reduction methods as well as grafting will be included in these approaches. As for the more traditional methods, the spontaneous functionalization of carbon with redox active moieties through diazonium chemistry has been extensively studied with the motivation to add a pseudocapacitive contribution to the double layer capacitance [28–31].

To understand the effect of surface chemistry on the reactivity of the carbon surface, a detailed understanding of the degradation of the carbon/electrolyte interface during charging of the supercapacitor is required. For this purpose, the gas evolution during charging, discharging and aging of a symmetric carbon/carbon supercapacitor in a sulfate-based aqueous electrolyte will be followed operando by coupling a mass spectrometer to the electrochemical cell. A customized and fully automated setup will be used for the quantitative study of low gas generation electrochemical systems such as supercapacitors [4]. Differences observed in gas levels and compositions as a function of cell voltage can thus be correlated with the evolution of the physicochemical properties of the carbon electrodes and with the electrochemical performances to obtain a complete picture of the processes taking place at the electrode/electrolyte interface. Such a methodology reveals the influence of the different surface functionalities of the carbon electrodes on the reactions occurring at the electrode/electrolyte interface and allows the tailoring of the electrode material at the positive and negative electrodes to improve the cell voltage. An asymmetric supercapacitor configuration with an extended operating voltage will be proposed.

2. Experimental

2.1. Carbon modifications

The surface functionality of a commercial porous carbon (Norit, DLC Super30), labelled AC, was modified using chemical oxidation, reduction with H_2 gas and chemical grafting.

Chemical oxidation was performed by dispersing the carbon powder (25 g) into a solution of nitric acid (Sigma Aldrich ACS reagent 70 % diluted at 10 mol L^{-1}, 500 mL). The mixture was heated up to 80 °C under stirring for 2 h. The oxidized carbon (named ACox) was abundantly washed with deionized water and dried in an oven at 80 °C overnight.

Reduction with H_2 gas was performed by heating the AC carbon up to 700 °C at 10 °C min^{-1} in a tubular furnace under 100 mL min^{-1} of a gas flow containing 5 % of H_2 in N_2. Afterwards the temperature was kept at 700 °C during 1 h under the same gas flow/composition. The material collected after cooling down the furnace under a N_2 flow of 100 mL min^{-1} was named ACH_2.

The diazonium reduction technique was used for the chemical grafting of benzoic acid and phenyl groups to the carbon surface (samples named AC-Ph-COOH and AC-Ph-H, respectively). The reaction was conducted by dispersing 5 g of AC in hydrochloric acid solution (Sigma Aldrich ACS reagent 37 % diluted at 0.5 mol, 150 mL) using magnetic stirrer. For the AC-Ph-COOH, the 4-aminobenzoic acid precursor was added in the solution (4.2 mmol, 0.01 molar equivalent toward carbon, Alfa Aesar, 97 %) followed by sodium nitrite (8.4 mmol, Sigma Aldrich, 97 %) to generate the diazonium cations. For the AC-Ph-H, the same procedure was used with aniline as precursor (4.2 mmol, 0.01 molar equivalent toward carbon, Alfa Aesar, 99 %). In both cases, the mixture were stirred for 12 h at ambient temperature, filtered, and washed successively with deionized water (3 x 50 mL), dimethylformamide (3 x 100 mL), ethanol (3 x 50 mL) and acetone (3 x 50 mL). The powder was then dried overnight at 80 °C.

2.2. Electrode preparation

Two different kinds of electrodes have been prepared with the pristine and the modified carbons; self-standing and coated films over metallic current collectors. Self-standing electrodes were prepared by mixing, in a small volume of ethanol: i) carbon (80 wt%), ii) acetylene carbon black (10 wt%, Timcal Super C65) used as conductive material and, iii) polytetrafluoroethylene, PTFE, (10 wt%, dispersion in water from Aldrich) used as binder. The mixture was stirred until a homogenized paste-like consistency was obtained. The paste was cold rolled and was dried overnight in an oven at a temperature of 80 °C. The electrodes were then cut into disks of 10 mm diameter for being used in Swagelok® cells.

Film electrodes over stainless steel foils were prepared by mixing: i) active materials (85 wt%), ii) acetylene carbon black (5 wt%, Timcal Super C65) and polyvinylidene fluoride binder, PVDF (10 wt%, Solex from Solvay) in N-methylpyrrolidone solvent. The mixture was then homogenized using IKA Ultra-Turrax device (T-25 Digital) for 20 min. This slurry was casted onto a stainless steel foil (10 μm thickness) with

Elcometer 4340 system at a temperature of 100 °C. The different electrodes were calendared and then dried at 80 °C overnight. Average thickness of the carbon films was 100 μm with a density of 0.875 g cm^{-3}. The films were cut into 5 x 4 cm^{-1} electrodes to be used in the cell coupled to the mass spectrometer.

2.3. Electrochemical characterization

Electrochemical characterization was performed with two- and three-electrode Swagelok® cells by cyclic voltammetry (2 mV s^{-1}), galvanostatic charge/discharge (0.2–10 A g^{-1}), voltage floating and impedance spectroscopy by using MPG-2 and VMP3 multichannel potentiostats/galvanostats (Biologic, France). A three-electrode configuration was used in a one-compartment (3 mL) Swagelok® cell for the electrochemical characterization of the carbon based electrodes. The counter electrode was a graphite rod and a Hg/Hg_2SO_4 was used at reference electrode. Two-electrode Teflon Swagelok® cells were assembled with 10 mm diameter carbon electrodes over stainless steel current collectors, and glass fiber paper (Whatman®, thickness 670 μm) was used as a separator. An Ag/AgCl reference electrode was added to the two-electrode Teflon Swagelok® cells for monitoring electrode potentials during two-electrode cell operation. The electrolyte (Li_2SO_4, 2 mol L^{-1}) was degassed before mounting the cells under helium at room temperature. All potentials are referred to NHE electrode. Prior to any measurement, the working electrode was dipped in the electrolyte for 20 min in order to allow the electrolyte to impregnate the electrode porosity.

Ageing tests of carbon/carbon capacitors were performed by voltage floating using a custom-built airtight and compact electrochemical cell with 20 cm^2 electrodes. Gas evolution was monitored operando by pulsed electrochemical mass spectrometry (PEMS) using the protocol described elsewhere [4]. Various valves and flowmeters were synchronised with the potentiostat/galvanostat (SP-50, Biologic, France) using in-house developed software to transport the gases to a mass spectrometer (QMS 403C Aeolos, Netzsch, Germany) at the desired time during cell operation. Prior to ageing of the supercapacitor, the electrodes were conditioned by a series of galvanostatic cycles (0.5 A g^{-1}) with a gradually increasing voltage from 1.0 V to 2.0 V. After conditioning, ageing consisted of a 50 h float. At each hour of float, the gas was sampled from the cell and the capacity measured after five cycles of galvanostatic charge-discharge at 0.5 A g^{-1}. Additional ageing tests at 10 and 20 h were performed to characterize the evolution of the physico-chemical properties of the electrodes during ageing.

2.4. Physicochemical characterization

2.4.1. Porous texture

The specific surface area measurements were conducted on a Quadrasorb-evo (Quantachrome Instrument, USA) at 77 K and the QuadraWin software was used for data analysis. Before the measurement, samples (50–70 mg) were outgassed for overnight under vacuum at 120 °C. The specific surface area (SSA) was evaluated from the N_2 adsorption isotherm using the Brunauer-Emmett-Teller (BET) equation.

2.4.2. Surface chemistry

Temperature programmed desorption (TPD) was used to analyze the surface functionalities of raw carbons and carbon electrodes at different aging times. Samples (10–15 mg) were placed in an STA 449C Thermobalance (Netzsch, Germany) coupled to mass spectrometer (QMS 403C Aeolos, Netzsch, Germany) and kept at room temperature for 1 h under an helium flow of 100 mL min^{-1}. The temperature was then raised up to 1200 °C at a rate of 10 °C min^{-1} under a flow of helium of 100 mL min^{-1}. The decomposition products of the samples were detected by online mass spectrometry.

X-ray photo-electron spectra (XPS) on carbon powder were recorded with a VG ESCALAB 250 spectrometer using an Al Kα monochromatic source (15 kV, 15 mA) and a multi-detection analyzer, under 10^{-8} Pa residual pressure.

The pH corresponding to the point of zero charge (pH_{PZC}) was used to determine the nature of the carbon surface. This was measured by the mass titration method. The carbon was dispersed in a suitable volume of distilled water with carbon water ratios from 1 to 16 w/w and kept under constant stirring in a nitrogen atmosphere at room temperature until equilibrium was reached (approximately 48 h). The pH_{PZC} value of the material corresponded to the plateau in the plot of equilibrium pH versus solid weight fraction [32].

3. Results and discussion

3.1. Effect of oxygen surface functionalities on electrochemical performance

Following previous studies [2,23], the first strategy followed to protect the electrodes from the electrochemical degradation was to introduce oxygenated surface functionalities at the carbon surface. The oxygen functionalities have been introduced in the carbon surface by chemical oxidation using nitric acid (ACox) and by chemical grafting (AC-Ph-COOH). For the chemical grafting, the choice of a carboxyl group as functionality has been done in order to decrease the pH at the electrode/electrolyte interface. Carboxyl groups (-COOH) in contact with an almost neutral electrolyte as 2 mol L^{-1} Li_2SO_4 with a pH of around 6 are able to give rise to negative charges on the carbon surface and to H^+ ($-COO^- + H^+$) decreasing the local pH of the carbon surface.

3.1.1. Physicochemical characterization of as-received and modified carbons

In order to study the effect of both oxidation methods on the surface functionality of the AC carbon, Fig. 1 presents the TPD-MS profiles obtained for the pristine and the oxidized carbons. The total amount of O-containing groups was found of 1.0, 9.0 and 4.0 wt % for AC, ACox and AC-Ph-COOH, respectively, showing the effectiveness of the selected oxidation treatments.

Carbon material AC revealed a rather low oxidation degree, as inferred from the low total mass loss ca. 2 % and low amount of CO desorbed, between 600 °C and 1000 °C, corresponding to the presence of phenolic or ether like groups. After an acidic treatment, sample ACox showed a mass loss of ca. 15 % revealing the presence of a big amount of oxygen surface functionalities. The CO_2 gas evolution arises in a large range of temperatures from 200 °C to 800 °C, indicating the presence of a large amount of carboxylic acids, carboxylic anhydrides and lactones. Similarly, the CO evolved between 200 °C and 1000 °C arising from the decomposition of carboxylic acid, carboxylic anhydride, phenol and carbonyl/quinone groups. These results show the non-selective oxidation of the surface through the followed chemical oxidation treatment. By contrast, the oxidation treatment consisting in a chemical grafting of benzoic acid groups (AC-Ph-COOH) derives to desorption of CO_2 and CO in a narrower temperature range despite the total mass loss was found as ca. 10 %. Both profiles showed a wide peak at 100–300 °C associated to the presence of carboxylic acids, followed by a narrow peak between 300 °C and 500 °C assigned to decomposition of carboxylic anhydrides. Scheme 1 illustrates the effect of the two oxidation methods on the oxygen surface functionalities of the AC carbon.

These results have been confirmed by XPS. Table 1 summarizes the amount and the nature of the O-containing functionalities. The XPS experiments revels that only functionalities related with carboxylic bonding can be found for the grafted carbon, while all types of functionalities were detected for the chemically oxidized one. It is noteworthy that while the oxygen content obtained by both techniques for AC and ACox is comparable, the amount found by XPS for the sample AC-Ph-COOH is twice that revealed by TPD-MS. This indicates that in this sample, the oxygenated groups are predominantly located on the external surface of the material, as the quantification provided by XPS

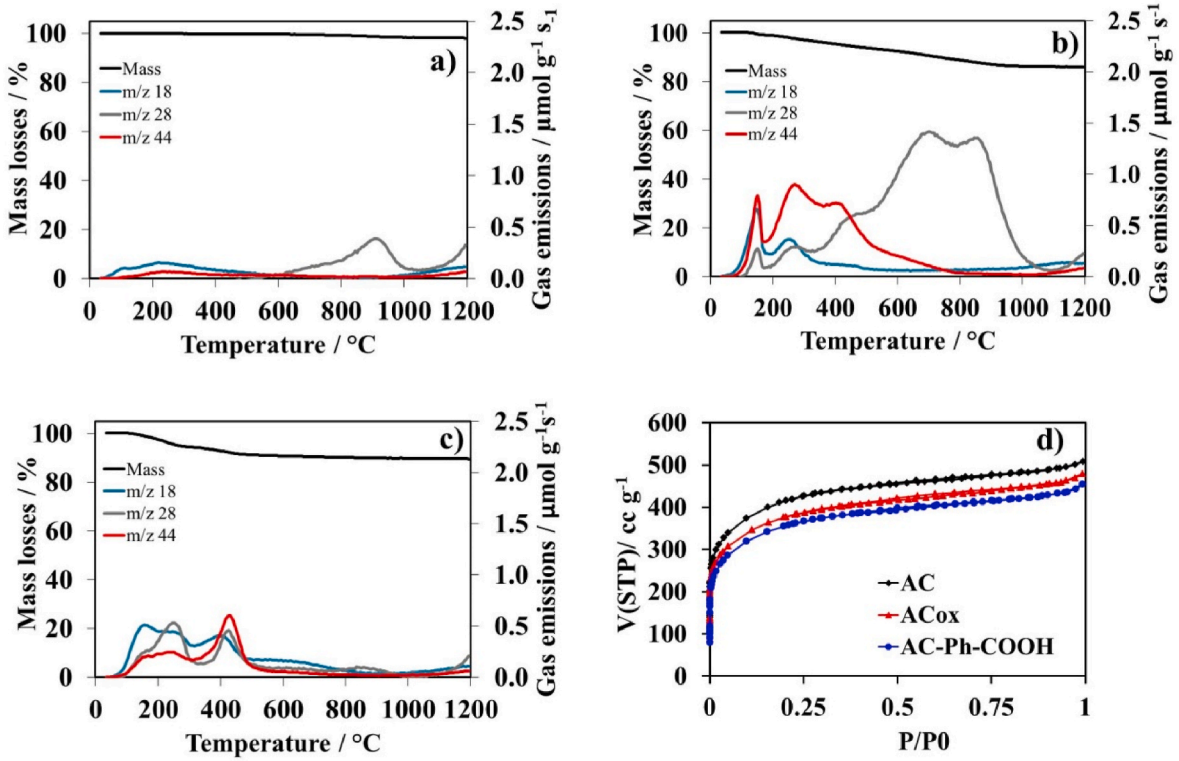

Fig. 1. Profiles of mass loss and gas evolved from TPD-MS corresponding to *m/z* 18 (H_2O), 28 (CO) and 44 (CO_2) signals for AC (a), AC_{OX} (b) and AC-Ph-COOH (c). N_2 adsorption isotherms for AC, AC_{ox} and AC-Ph-COOH (d).

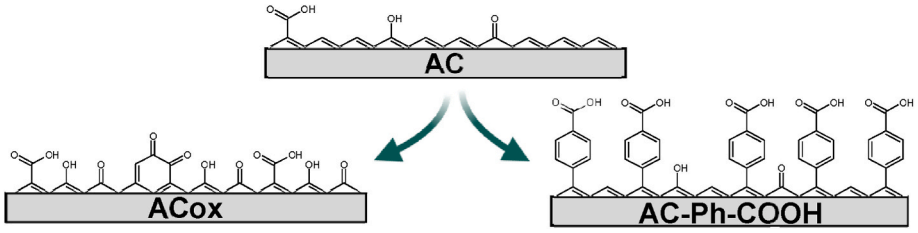

Scheme 1. Surface functionalities of AC, ACox and AC-Ph-COOH carbons.

Table 1
O-containing amount obtained by TPD-MS and XPS analysis of surface functionalities nature. pH of PZC and specific surface area calculated from N_2 adsorption isotherm at 77 K.

Material	O wt. % (TPD-MS)	pH_{PZC}	O at. % (XPS)	C-OR at. %	C═O at. %	-*O*-C═O at. %	SSA $m^2 g^{-1}$
AC	1.0	7.5	1.1	1.1	–	–	1400
ACox	9.1	2.4	9.7	3.0	1.8	2.4	1240
AC-Ph-COOH	4.0	3.0	7.9	2.7	–	2.5	1180

corresponds to the most external surface of the carbon, while TPD analysis accounts for the total oxygen content. In fact, it is known that chemical grafting can lead to a dramatic decrease in SSA caused by the accumulation of molecules at the entrance of the micropores [30,31]. Therefore, in order not to decrease the double layer capacitance of the carbons, it is necessary not to affect the porosity much during the surface modification process.

In this sense, Fig. 1d and Table 1 show that both oxidation treatments have a small effect on the SSA and the pore volume compared to the raw carbon. In fact, for the specific case of the grafting method, different amounts of precursor were tested, from 0.1 to 0.01 molar equivalents of carbon, in order to find the best compromise between functionalization and preservation of the porous texture. Since the use of 0.1 molar equivalents results in a 23 % decrease in SSA, 0.01 molar equivalents results in a slight porosity block with only a 15 % decrease in SSA (Table 1). Finally, the amount was limited to 0.01 to avoid the formation of multilayers at the pore entrances. These results show that a large amount of oxygen can be selectively introduced into the carbon surface without blocking the pores by controlling the precursor concentration.

The augmentation of oxygen content on the carbon surface was also reflected on surface pH, which suffered a noticeable fall after both oxidation treatments (Table 1). The raw carbon has a neutral nature while the oxidized carbons present an acidic one with pH_{PZC} of 2.4 and 3.0 for the ACox and the AC-Ph-COOH, respectively.

3.1.2. Effect of oxygen functionalities on carbon electrochemical performance

Fig. 2a shows the cyclic voltammetry of the pristine and modified materials carried out in a three-electrode cell in an aqueous electrolyte as Li2SO4. All materials showed a quasi-rectangular shape ascribed to the double layer capacitance contribution of the porous carbons. The chemical grafted carbon presented a slightly lower electrical double

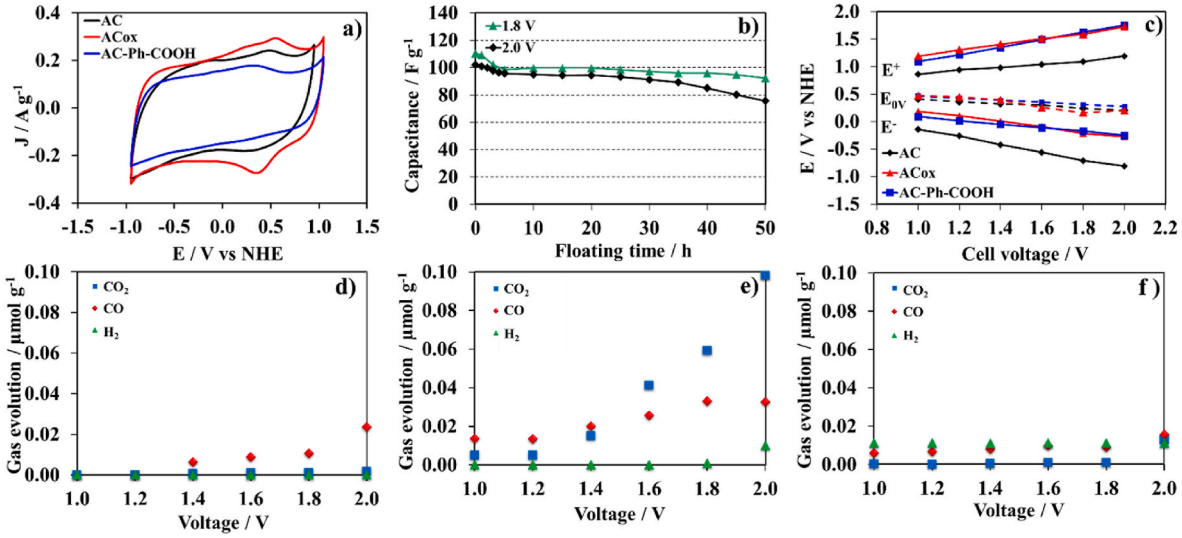

Fig. 2. Cyclic voltammograms recorded in a three-electrode cell at 2 mV s^{-1} in 2 mol L^{-1} Li_2SO_4 of three studied materials. Fifth scan recorded (a). Capacitance evolution as function of floating time at 1.8 and 2.0 V for symmetric AC/AC supercapacitor (b). Potential limits of positive (E^+) and negative (E^-) electrodes during cycling from 1.0 to 2.0 V of symmetric supercapacitors in 2 mol L^{-1} Li_2SO_4. The E_{0V} values (dashed lines) correspond to the electrodes potential when the cell voltage is shifted to 0.0 V before each change of maximum voltage (c). Amount of gas released during polarization when cell voltage is increased from 1.0V to 2.0V in symmetric supercapacitors manufactured by AC (d), AC_{OX} (e), and AC-Ph-COOH (f).

layer capacitance in line with the lower specific surface area. The voltammograms revealed the presence of redox reversible humps related to the pseudo-faradic reactions involving oxygen functional groups, at the potential range between 0.0 and 0.6 V vs. NHE, being much more remarkable for the sample ACox. Moreover, the presence of those O-containing groups in oxidized samples also influences the capacitive response, as the voltammograms for the ACox and the AC-Ph-COOH carbons display more rectangular shape than the AC, presumably linked to a higher surface wettability.

The common feature related to the two oxidized carbons is the positive effect of the operating potential window. Either a chemical oxidized carbon or the grafted one, push the limit for positive polarization to higher values (up to 1.1 V vs NHE). This could be associated to the decrease of the local pH at the interface electrode/electrolyte. In fact, since the pH of the electrolyte is higher than the pH_{PZC} of the modified carbons, functionalities as carboxyl groups and lactones will give rise to negative charges and H^+ [33]. This decrease in pH at the interface would shift the thermodynamic potentials for water splitting to higher values according to Nerst's law. These results indicate that modified carbon materials require a higher potential to be oxidized than the original.

3.1.3. *Effect of oxygen functionalities on supercapacitor operation*

Symmetric supercapacitors have been built with the pristine or the modified carbons in order to assess the effect of the oxygen functionalities on the ageing of the system. For the purpose of establishing aging conditions, Fig. 2b shows the capacitance retention for the pristine carbon-based supercapacitor during floating tests at 1.8 V and 2.0 V. The Figure shows a similar initial decrease of capacitance during the first hours, followed by a capacitance plateau. At 2.0 V, after 20 h floating, there is a sharp decrease of capacitance to reach a capacitance loss of 26 %. However, at 1.8 V, the capacitance is maintained throughout the floating experiment, with only a slight decrease, less than 5 F g^{-1}, observed over 40 h of floating. These results confirm that 2.0 V is a too high cell voltage for the symmetric AC/AC supercapacitor. Nevertheless, a floating voltage of 2.0 V has been chosen to compare with the modified carbon based supercapacitors in order to perform accelerated ageing tests and to explore the possibility to increase the cell voltage by modifying the surface chemistry of the carbon materials.

Before reaching the floating voltage, the supercapacitors were gradually polarized from 1.0 V to 2.0 V performing some galvanostatic charge discharge cycles every 0.2 V. To analyze the behavior of the electrodes during this cell conditioning, the potential window of each electrode was recorded by a reference electrode introduced into the electrochemical cell while the symmetric carbon/carbon supercapacitor was polarized. Fig. 2c shows the evolution of the potential measured at cell voltage of 0 V, denoted as E_{0V}, and the measured potential of the positive (E^+) and negative (E^-) electrodes, for the supercapacitors built using AC, ACox or AC-Ph-COOH electrodes. In the case of the supercapacitor assembled with the non-modified carbon, the operating potential range of the positive and negative electrode (ΔE^+ and ΔE^-, respectively) has the same extension for any cell voltage from 1.0 to 2.0 V. However, for the supercapacitor built with the modified carbons the operation of the electrodes during cell polarization is completely different. From one side, all the potentials are shifted to higher values corresponding to the increase of the local pH at the carbon/electrolyte interface as discussed above. From the other side, there is an important disymmetrization of the electrodes operating potential windows. For the ACox and the AC-Ph-COOH based supercapacitors, the ΔE^+ is much wider than the ΔE^- indicating a higher capacitance of the negative electrode than the positive one. Therefore, the maximum potential reached by the positive electrode during the supercapacitor operation is still shifted to higher values. Consequently, when the carbon material contains surface oxygenated groups, the positive electrode in the supercapacitor operates beyond oxygen evolution limit found in the voltammetry (ca. 1.1 V vs NHE, Fig. 2a). However, in the case of the negative electrode, all materials showed a potential far to reach that required for the H_2 evolution reaction (ca. −1.0 V NHE).

Aiming to analyze this behavior, Fig. 2d,e,f show the evolution of gases during the polarization of the different supercapacitors from 1.0 to 2.0 V. In concordance with Fig. 2c, H_2 was not detected at any voltage since the negative electrode is not reaching the H_2 evolution limit. For the AC carbon based supercapacitor, there is a small evolution of CO increasing with the cell voltage above 1.4 V, in line with the beginning of an electrochemical oxidation of the carbon at the positive electrode following the previously reported mechanism [4]. For the chemically oxidized carbon based supercapacitors there is a considerable amount of gases evolving as CO and CO_2 in all voltage range. These gases are associated with either the decomposition of unstable oxygen surface functionalities or the operation of the positive electrode at a potential

where the carbon is electrochemically oxidized. However, in the case of the grafted carbon based capacitor, even if the potential of the positive electrode is as high as for the chemical oxidized carbon (ranged from 1.4 to 2.0 V vs. NHE), the amount of gases related with a possible oxidation of carbon is very low. Such results could indicate that the grafted molecules at the surface of the carbon might in somehow protect the surface from an electrochemical oxidation.

However, only an ageing experiment by floating at high voltage can confirm that the modification of the carbon surface is preserving the positive electrode to be oxidized. Fig. 3 presents the evolution of the capacitance for the symmetric capacitors built with the as-received and the modified carbons during 50 h floating at a cell voltage of 2.0 V. During the first 5 h of voltage floating, the capacitance retention of the three supercapacitors was similar with a capacitance decrease of around 8 %. For the ACox carbon based supercapacitor, beyond 5 h the capacitance continues to sharply decrease reaching a 15 % loss after 10 h floating, but, during the next hours of ageing, the capacitance loss is slower reaching a value of 23 % after 50 h floating. Despite this material avoids the sharp capacitance decrease observed after only 20 h for the non-modified electrodes, its capacitance retention is still too low to consider 2.0 V as a reliable cell voltage. However, when AC-Ph-COOH is used as electrode, the capacitance decreases by 10 % after 10 h of aging and only a further 5 % is lost after 50 h of floating. These results indicate that AC-Ph-COOH material allows the operation of the supercapacitor at a cell voltage of 2.0 V for long time with a capacitance retention higher than 83 %. Therefore, modifying the carbon surface by grafting a given oxygen surface functionality seems to be somehow more efficient than chemical oxidation to avoid irreversible reactions at the electrode/electrolyte interface responsible for the capacitance loss.

The evolution of gases during the floating experiments has been followed by PEMS in order to give insights on the interface reactions at the origin of ageing. The evolution of H_2, CO and CO_2 has been monitored every hour of floating at 2.0 V for the three different supercapacitors as it is presented in Fig. 4a and b and c. Results show that for all materials, the gases evolving during ageing are mainly CO_2 and H_2, followed by small amounts of CO. As it has been previously discussed [4], CO_2 is a precise indicator of the positive electrode aging while H_2 is related with the decomposition of the electrolyte at the negative electrode. For the non-modified material based supercapacitor, at the beginning of the ageing experiment (below ca. 3 h) the only released gas is CO (Fig. 4a) as a continuation of the gases evolved during previous cell voltage increase (Fig. 2c). After a few hours of floating, CO is no longer evolved, but an increase in CO_2 release is observed, since at high voltages the oxidation of carbon causes more O-rich functionalities to desorb preferentially as CO_2 [4]. This CO_2 evolution reaches its maximum at 40 h, followed by an abrupt decrease during the last hours of floating. To understand this behavior, Fig. 4d shows the electrode potentials (E^+, E^- and E_{0V}) registered every hour during the floating experiments. Although the maximum potential reached by the positive electrode (E^+) decreases during the first hours of floating, the important evolution of CO_2 indicates that such potential is still too high to avoid the oxidation of the electrode. The variation of the potentials is directly related with modifications in the physico-chemical properties of carbon materials while keeping the cell voltage at 2.0 V. Indeed, Fig. 4g shows a continuous oxidation of the positive electrode with an increase on the oxygen surface content from 7.5 wt% to 20 wt% after 50 h voltage floating. In addition, an abrupt decrease in the surface area of the positive electrode is observed. After 20 h ageing, the SSA is reduced by a factor of 10, indicating that such oxidation of the carbon leads to a collapse of the porosity. Conversely, the decrease in the potential of the negative electrode during the first hours of floating (Fig. 4d) leads to a small release of hydrogen without a significant impact on the specific surface area of the electrode (Fig. 4g). Thus, the reason for the decrease in capacitance observed in Fig. 3 is primarily related to the loss of capacitance of the positive electrode due to the effect of oxidation on the porosity.

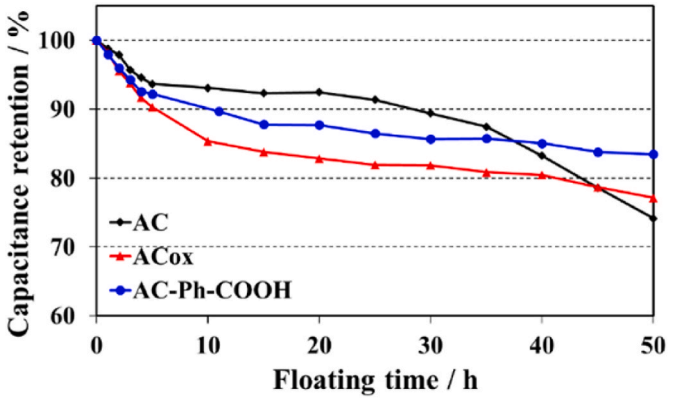

Fig. 3. Evolution of capacitance retention as a function of floating time at 2.0 V in 2 mol L^{-1} Li_2SO_4, for symmetric supercapacitors built with AC, AC_{OX} and AC-Ph-COOH.

The same experiments were carried out with the supercapacitors assembled with the surface modified materials. Fig. 4b shows that for the supercapacitor with the electrodes on chemically oxidized carbon, the amount of released CO_2 is very extensive at the beginning of the floating experiment. Actually, the high CO_2 levels at the beginning of the floating experience correspond to the ones found at the end of the cell conditioning to reach 2.0 V (Fig. 2c). The significant CO_2 evolution can be related either to the desorption of functional groups present in the ACox carbon or to further electrochemical oxidation, and is consistent with the rapid capacity loss obtained during the first hour of floating (Fig. 3b). However, the amount of CO_2 evolved decrease rapidly during the first hours of ageing and in a more moderated manner up to the end of the experience. The decrease in CO_2 release can be easily related to the decrease in the maximum potential reached by the positive electrode during the first hours of voltage floating, as observed in Fig. 4e. Nevertheless, the potential seems to stabilize at a too high value, even if the low pHpzc of the carbon after functionalization leads to an increase in the carbon oxidation potential. In fact, Fig. 4h shows an increase in the surface oxygen content from 11.1 wt% to 21.0 wt% after only 10 h of floating. Thereafter, there is no further increase in the oxygen content, but the continuous evolution of CO_2 is an indication of a continuous oxidation of the carbon. This oxidation implies a reduction in the mass of the positive electrode and a decrease in the electrode porosity (Fig. 4h). Although the ACox positive electrode maintains a slightly higher surface area than the unmodified one after 50 h, allowing the system to retain 78 % of its capacity, the non-selective carbon oxidation seems insufficient to prevent further electrochemical oxidation. However, Fig. 4h shows that the porosity of the negative electrode has not changed during ageing. Thus, like the AC supercapacitor, this oxidation of the carbon material at the positive electrode limits the operating cell voltage.

In contrast, the AC-Ph-COOH based supercapacitor shows a different picture; Fig. 4c shows a small amount of CO_2 released throughout the ageing process. Fig. 4i shows that during the first 20 h of floating, the amount of oxygen at the carbon surface of the positive electrode increases from 5.6 wt% to 15.9 wt% with a small effect of the specific surface area. The electrode potentials then stabilize at a value approximately 120 mV lower than that of the oxidized carbon supercapacitor (Fig. 4f). These lower electrode potentials, together with the effect of the pH_{PZC} on the oxidation potential, are consistent with the lower CO_2 evolution shown during the floating experiment. After 20 h of floating, the oxygen content is no longer increasing and the decrease in SSA is less than for the AC or ACox positive electrodes. Therefore, the smaller extent of oxidation of the positive electrode results in the better capacitance retention observed in Fig. 3 for the AC-Ph-COOH based supercapacitor.

In summary, the results confirm that the positive electrode is the one that limits the operating voltage of the supercapacitor. Otherwise, the

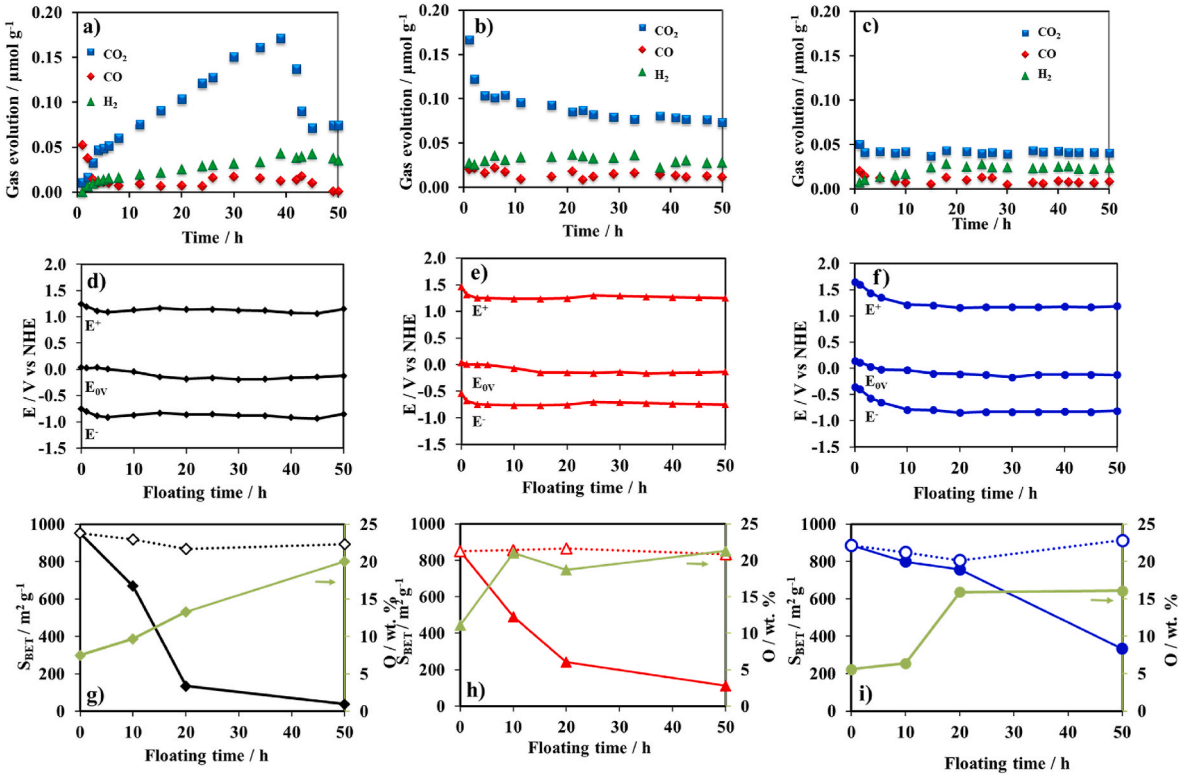

Fig. 4. Evolved gases amount as function of floating time at 2.0 V of symmetric supercapacitors built by AC (a), AC_{OX} (b), and AC-Ph-COOH (c). Potential limits of positive (E^+) and negative (E^-) electrodes during floating time at 2.0 V in 2 mol L^{-1} Li_2SO_4 of symmetric supercapacitors built by AC (d), AC_{OX} (e), and AC-Ph-COOH (f). The E_{0V} values corresponds to the electrodes potential when the cell voltage reaches 0.0 V. Correlation of SSA of the positive electrode (full lines) and the negative electrode (dashed lines) and O_2 wt. % of the positive electrode with selected floating times of symmetric supercapacitors built by AC (g), AC_{OX} (h), and AC-Ph-COOH (i).

grafting of an oxygen functionality as –COOH seems to be a valuable strategy to protect the positive electrode from oxidation in order to increase the cell voltage. Besides lowering the pH_{PZC} to increase the carbon limiting potential, the grafted functionalities seem to protect the carbon from further oxidation.

3.2. *Effect of H related surface functionalities on the electrochemical performance*

In order to understand whether the improvement in performance is a consequence of the selective introduction of oxygen functionalities as –COOH or because of the effect of grafting on the saturation of oxidation active sites at the carbon surface, a bare phenyl group was chemically grafted onto the AC carbon surface (sample AC-Ph-H). As it was described above, the grafting method used is a chemical one in which aryl radicals combine with active sites of the graphene layers of carbons through a covalent bond [28]. Therefore, for comparison purposes, the AC carbon has been also treated in a H_2 atmosphere at 700 °C (sample ACH_2). A thermal H_2 treatment is known to be efficient to remove surface oxygen to leave a basic stable surface nearly free of highly energetic sites with unpaired electrons capable to adsorb oxygen even at ambient temperature [34]. Scheme 2 illustrates the surface functionalization of the materials after treatment.

3.2.1. *Physicochemical and electrochemical characterization of H-based carbons*

Fig. 5 and Table 2 presents the results of the physicochemical characterisation of the H-based materials. The table shows that the specific surface area obtained from the N_2 adsorption isotherm presented in Fig. 5a of the AC-Ph-H carbon after phenyl grafting is only slightly less than that of the raw carbon. Indeed, the amount of phenyl precursor was modulated to do not block the porosity. Moreover, during the chemical grafting reaction in the liquid phase, there is a slight oxidation of the carbon surface as 2.4 wt% of oxygen was found by TPD-MS (Fig. 5b). For the ACH_2 material, the H_2 treatment does not significantly change the specific surface area of the carbon as seen in the N_2 adsorption isotherm in Fig. 5a and the amount of oxygen in the surface obtained by TPD-MS (Fig. 5c) is now less than 1.0 wt%. These two treatments have opposite effects on the pHpzc of the untreated carbon. Whereas hydrogen treatment leads to an increase in pHpzc up to 8.3 as a consequence of the

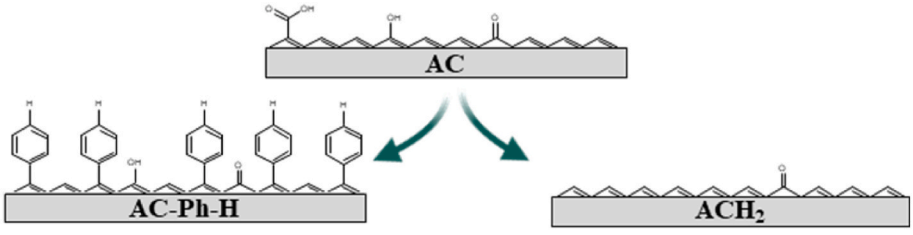

Scheme 2. Surface functionalities of AC, AC-Ph-H, and ACH_2 carbons.

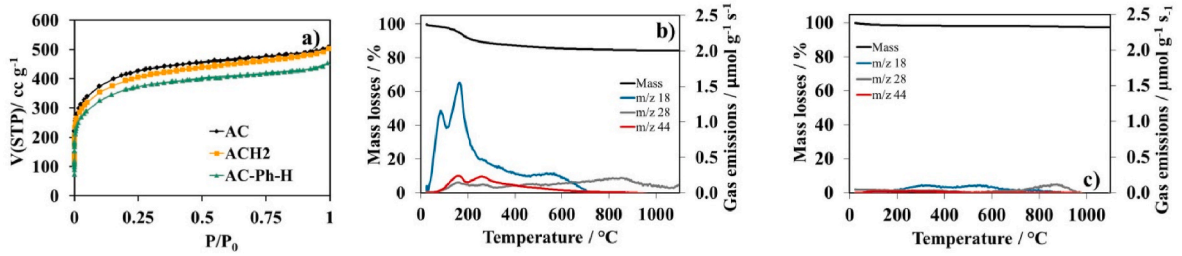

Fig. 5. N_2 adsorption isotherms for AC, ACH_2 and AC-Ph-COOH (a).Profiles of mass loss and gas evolved from TPD-MS corresponding to *m/z* 18 (H_2O), 28 (CO) and 44 (CO_2) signals for ACH_2 (b) and AC-Ph-H (c).

Table 2
O- amount obtained by TPD-MS, pH_{PZC} and specific surface area, calculated from N_2 adsorption isotherm at 77 K, of AC, ACH_2, and AC-Ph-H materials.

Material	O wt. % (TPD-MS)	pH_{PZC}	SSA $m^2\ g^{-1}$
AC	1.0	7.5	1400
AC-Ph-H	2.4	3.9	1230
ACH_2	0.8	8.3	1331

elimination of oxygen-containing groups [34], chemical grafting of a phenyl group leads to a decrease in pHpzc down to 3.9 as observed for the other modified carbon. Such a result suggests that the phenyl functionalities are also capable of generating negative charges on the carbon surface and H^+, thus lowering the local pH.

Fig. 6a shows the cyclic voltammetry of the two H-based materials and the raw carbon. The figure reveals an increase in the positive limit of polarization for AC-Ph-H towards 1.1 V vs. NHE compared to AC and ACH_2 (positive limit of 0.9 V vs. NHE). Such an increase is probably related to the lower pH at the carbon/electrolyte interface as a consequence of the lower pH_{PZC} of this material. In addition to the stability window, these treatments have an important effect on the electrochemical signature of the carbon material. A H_2 treatment increases the electrical conductivity of the carbon material as the voltammogram becomes more rectangular. In addition, very pronounced peaks in the range of 0.0–0.7 V vs. NHE are observed, related to pseudo-faradic reactions involving surface oxygenated groups. This indicates the rapid oxidation of the material during polarization. The extensive oxidation of this material is also favored by the high pH_{PZC}, which reduces the oxidation potential of carbon. This indicates the inefficiency of the H_2 treatment in protecting the carbon surface against oxidation.

These results are consistent with previous studies of oxygen adsorption on H_2-treated carbons. In fact, a H_2 treatment at high temperature was shown to be effective in removing high energy sites with unpaired electrons capable of adsorbing O_2 to generate oxygen surface functionalities at ambient temperature, since this was not the case for the edge sites of the graphene layers that adsorbed oxygen at higher temperatures [34]. Thus, it can be imagined that a high potential is sufficient to overcome the energetic barrier for these non-stabilized sites to react.

However, for the phenyl grafted carbon, the charging mechanism is mainly the EDL, as redox peaks are not appreciated. These results could indicate that the phenyl moieties have been grafted to those edge active sites for the electro-oxidation of the carbon.

3.2.2. *Effect of H related surface functionalities on supercapacitor operation*

Carbon/carbon symmetric capacitors were assembled using the H-based materials to assess the effect of these functionalities on ageing.

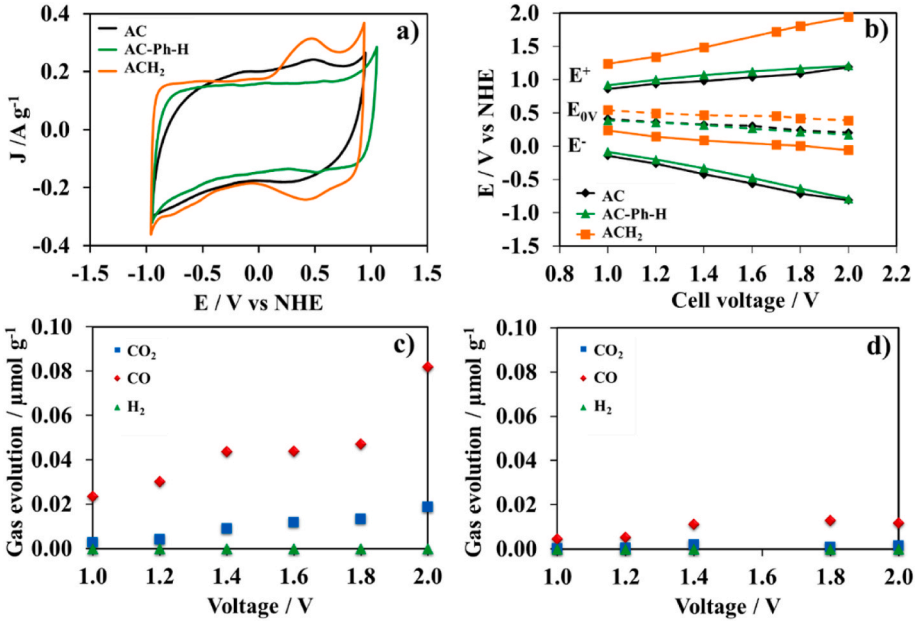

Fig. 6. Cyclic voltammograms of AC, AC-Ph-H, and ACH_2 materials recorded in a three-electrode cell at 2 mV s^{-1} in 2 mol L^{-1} Li_2SO_4. Fifth scan recorded (a). Potential limits of positive (E^+) and negative (E^-) electrodes during cycling from 1.0 to 2.0 V of AC, AC-Ph-H, and ACH_2 based symmetric supercapacitors in 2 mol L^{-1} Li_2SO_4. The E_{0V} values (dashed lines) correspond to the electrodes potential when the working voltage is shifted to 0 V before each change of maximum voltage (b). Evolved gases amounts while polarization from 1.0 V to 2.0 V of symmetric supercapacitors built by ACH_2 (c), and AC-Ph-H (d).

Again, the cell voltage was fixed at 2.0 V for the floating ageing experiments.

Prior to floating, Fig. 6b shows the evolution of the potential of the electrodes during the polarization of the symmetric configuration from a cell voltage increasing from 1.0 V to 2.0 V using AC-Ph-H or ACH_2 carbons as electrodes. The results for the AC based capacitors are shown for comparison. For the ACH_2 carbon supercapacitor, the loss of symmetry of the operating potential ranges compared to the raw carbon should be due to the extensive oxidation of the material during polarization observed in Fig. 6a. Fig. 6b shows that the negative electrode operates in the potential range where the redox reaction takes place, resulting in a much higher capacitance than the positive electrode. Therefore, in order to maintain charge equivalence between the two electrodes, the positive electrode operates in a wider potential window and the maximum potential reached by the electrode is outside the stability window of the carbon even at 1.0 V cell voltage. As a consequence, Fig. 6c shows the evolution of CO and CO_2 over the whole range of the cell voltage, resulting from the further electrochemical oxidation of the positive electrode, which increases exponentially at a cell voltage of 2.0 V.

In contrast, for the supercapacitor built with the AC-Ph-H electrodes, the operating potential window of both the negative and positive electrodes is similar at any cell voltage, in accordance with the EDL behaviour of this modified carbon (Fig. 6b). In fact, the maximum potential reached by the positive electrode during the polarization of the cell remains at the same level as that of the supercapacitor made with the non-modified carbon. The fact that both electrodes operate within their potential stability window is confirmed by the small amounts of gas evolved during the polarization of the cell from 1.0 V to 2.0 V, where only a few μmols of CO were detected above 1.4 V (Fig. 6d).

However, as discussed above, the effectiveness of a carbon surface modification in preventing oxidation of the positive electrode can only be evaluated through an ageing test. In this sense, Fig. 7a shows the capacitance retention of both materials -AC is included for comparison- over 50 h. The supercapacitor built with ACH_2 shows an excellent capacitance retention up to 15 h, after this floating time the capacitance starts to decrease progressively until reaching 82 % of the retention at 40 h, to finally decrease dramatically to a value of 45 % at 50 h. This behavior suggests that the extensive oxidation of the positive electrode, already observed during voltage conditioning to reach 2.0 V (Fig. 6c), continues during aging. This point is confirmed by the rapid increase of the evolved CO_2 during the first 15 h of floating (Fig. 7b). Although the maximum potential of the positive electrode decreases during the first hours of floating, the value remains well above the oxidation potential limit during the aging experience (Fig. 7c). Fig. 7b shows that the amount of evolved CO_2 suddenly decreases after the first 15 h of floating. This again indicates a collapse of the carbon surface area as the reason for the sudden capacitance loss observed in Fig. 7a. In fact, the SSA of the positive electrode after 50 h of floating was only 20 $m^2\ g^{-1}$. Therefore, it seems that hydrogen treatment does not deactivate the carbon surface sites to avoid further electrochemical oxidation during supercapacitor operation.

In contrast, the supercapacitor built with the carbon modified by chemical grafting of a phenyl group shows a much better capacitance

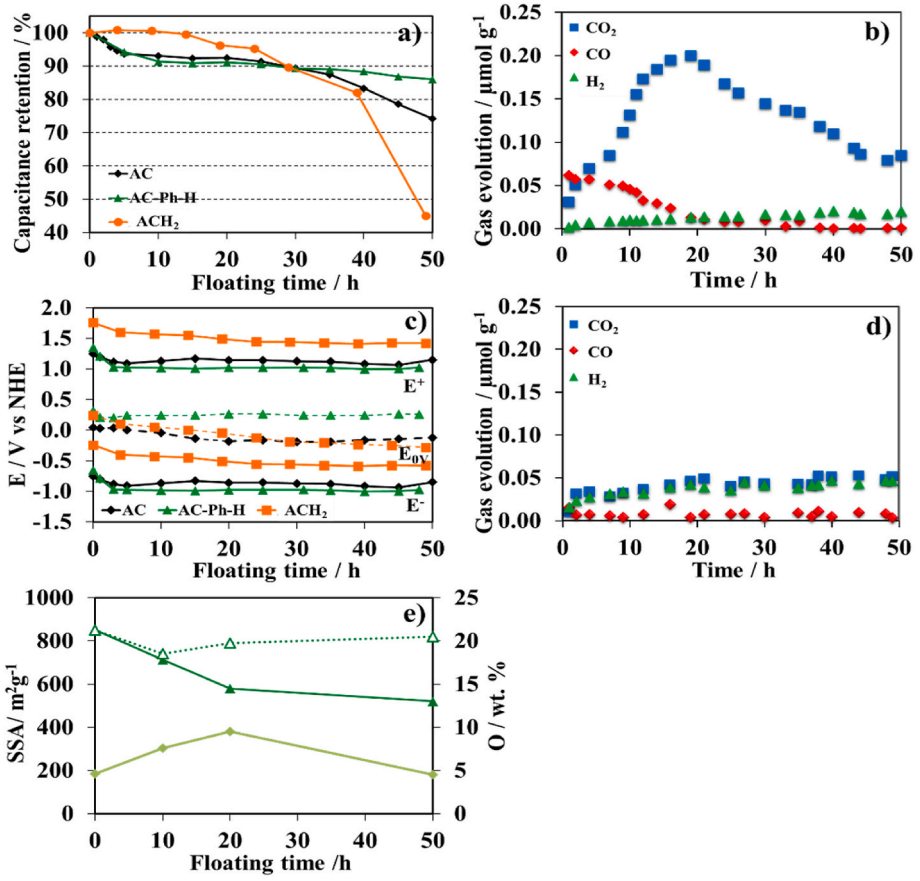

Fig. 7. Evolution of capacitance retention as a function of floating time at 2.0 V in 2 mol L^{-1} Li_2SO_4, for carbon based symmetric supercapacitors built with AC, AC-Ph-H, and ACH_2 (a). Evolved gases amounts as function of floating time at 2.0 V of symmetric supercapacitors built by ACH_2 (b). Potential limits of positive (E^+) and negative (E^-) electrodes during floating time at 2.0 V in 2 mol L^{-1} Li_2SO_4 of symmetric supercapacitors built by AC AC-Ph-H, and ACH_2. The E_{0V} values (dashed lines) correspond to the electrodes potential when the cel voltage is shifted to 0.0 V (c). Evolved gases amounts as function of floating time at 2.0 V of symmetric supercapacitors built by AC-Ph-H (d). Correlation of SSA of negative (dashed line) and positive (solid line) electrodes and O wt% of positive electrode with floating time at 2.0 V of symmetric AC-Ph-H/AC-Ph-H supercapacitor (e).

retention during the ageing experience (Fig. 7a). The capacitance shows a relatively fast decrease of about 10 % of the initial value during the first hours, similar to that observed for the pristine material supercapacitor, and then the decrease becomes very slow. This result points out that the oxidation of the positive electrode should not be very extensive. Fig. 7c shows that after a rapid decrease of the maximum potential reached by the positive electrode during the polarization of the cell up to 2.0 V, it stabilizes during the 50 h of floating at a value lower than that obtained for the supercapacitor with pristine AC carbon. Since the oxidation potential of the AC-Ph-H carbon is higher than that of the AC carbon due to its lower pH_{PZC}, this result indicates that the positive electrode remains below the oxidation potential when the supercapacitor operates at 2.0 V. The low evolution of gases during the float time (Fig. 7d) confirms the resistance of the positive electrode to oxidation. In addition, the analysis of the O content of the positive electrode shows a slight oxidation during the first hours of floating up to 20 h. The amount of oxygen on the carbon surface of the positive electrode increases from 4.6 wt% to 12.5 wt% during the first hours of floating and then decreases to the initial values. Then, the degree of oxygen functionalization during the ageing experiment is much lower than for the other positive electrodes made of raw or modified AC carbons. Consequently, the oxidation of the AC-Ph-H positive electrode has a smaller effect on the specific surface area than for the other supercapacitors studied and therefore on the capacitance loss. In fact, after 50 h of floating, the capacitance retention for the AC-Ph-H supercapacitor is 86 %, exceeding the 74 % obtained with the not modified carbon or even the 83 % obtained with the –COOH grafted material.

Finally, the better performance of the supercapacitors made with chemically grafted materials is related to the different behavior towards oxidation of the positive electrode during ageing at 2.0 V. To summarize, Fig. 8 shows the amount of surface oxygen obtained from the TPD experiments carried out on the positive electrodes made with the raw and modified materials after conditioning the cell up to 2.0 V (denoted as 0 h in the figure) and after 10, 20 and 50 h of voltage floating. The amount of surface oxygen from functionalities evolving as CO or CO_2 was normalised by the corresponding specific surface area of the electrode at the given aging time, considering that the porosity of the electrodes was modified during the aging (see Figs. 4 and 7). Fig. 8 a and b show that for the AC SC, the amount of oxygen fixed to the surface to generate oxygen functionalities desorbing as CO (Fig. 8a) or CO_2 (Fig. 8b) increases continuously from the first to the 50th hour of aging. These results indicate that the desorption of CO_2 observed for this supercapacitor during the ageing experiment (Fig. 4a) generates new sites for further oxidation, in addition to the large number of active oxidation sites initially present on the carbon surface. A chemical oxidation of the carbon prior to the assembly of the supercapacitor leads to a protection of the positive electrode surface, as the amount of surface oxygen is significantly lower for the ACox electrode. However, the continuous increase of the surface oxygen content during the ageing experiment is an indicator of the limited efficiency of such an approach. In contrast, the grafted materials have a significant oxidation resistance in comparison to the raw material. Fig. 8 a and b show that, compared to the AC positive electrode, the amounts of surface oxygen for the grafted materials are not visible even after 50 h of voltage floating at 2.0 V. To have a closer look at the comparison between the AC-Ph-COOH and the AC-Ph-H, Fig. 8 presents a zoom on the amount of oxygen fixed to form functionalities desorbing as CO (Fig. 8c) or CO_2 (Fig. 8d) from these two electrodes during the ageing of their corresponding symmetric capacitors. The figure shows a similar behavior during the first hours of floating, with a small increase of oxygen from functionalities desorbing as CO. As the extent of oxidation is very small, the typical carbon electrooxidation mechanism can be observed, initially producing groups that desorb as CO [4]. However, after 20 h of floating, since the AC-Ph-COOH electrode continues the extension of oxidation with the generation of a small amount of groups desorbing as CO_2, the AC-Ph-H does not present any further oxidation. In fact, the decrease in surface oxygen at the end of the ageing experience indicates that the small evolution of gases observed for the AC-Phi-H based supercapacitor (Fig. 7d) arise from the removing of the oxygen functionalities present in the surface without creating new active sites.

These results demonstrate that the grafted groups protect the electrode by blocking the active sites. This protection seems to be more efficient when the phenyl group covalently bonded to the active sites of the carbon does not contain an electron withdrawing functional group as a carboxylic acid. This active site blocking effect combined with decreasing the pH_{PZC} to increase the oxidation potential, results in an

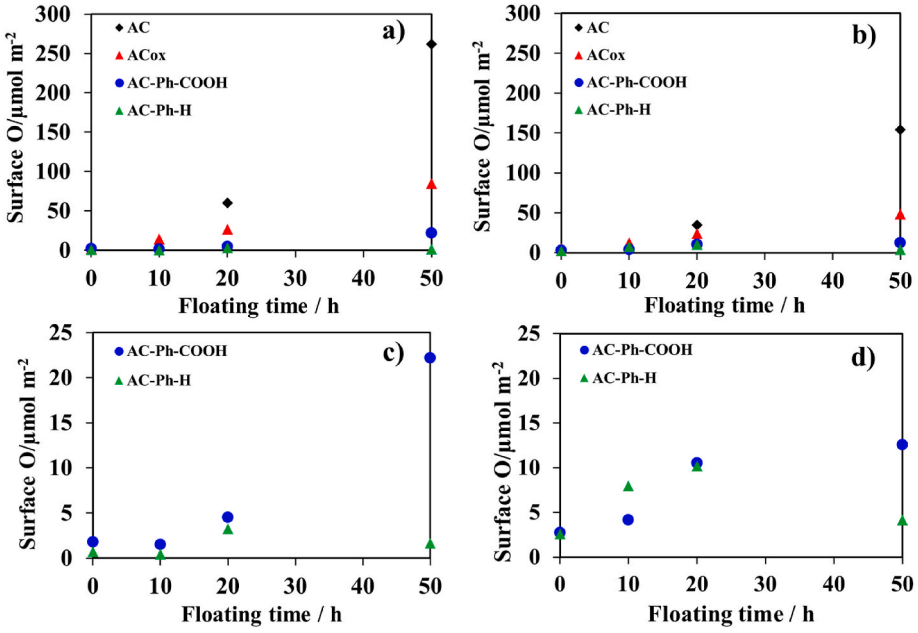

Fig. 8. Surface O amounts obtained from evolving CO (a) and CO_2 (b) by TPD-MS of the positive electrodes AC, ACox, AC-Ph-COOH, and AC-Ph-H after ageing the symmetric supercapacitors at 2.0 V at different times. Zoom of plots of surface oxygen calculated from evolving CO (c) and CO_2 (d) gases of AC-Ph-COOH and AC-Ph-H positive electrodes.

efficient strategy to protect the positive electrode from oxidation and therefore to increase the cell voltage and the energy stored.

However, as decreasing the pH_{PZC} also increases the potential for H_2 evolution, the potential reached by the negative electrode of the AC-Ph-H supercapacitor during ageing (Fig. 7c) is now close to the limit at which the H_2 is produced, as indicated by the small amount of H_2 evolved during the floating experiment (Fig. 7d).

Therefore, using the surface modified electrode on the negative electrode is not a good strategy to further increase the cell operation.

3.3. Electrochemical performance of asymmetric carbon/carbon supercapacitor

According to all the above results, an asymmetric system was assembled using the material with the best performance as positive electrode (AC-Ph-H) and the non-modified carbon as negative electrode.

The ageing behavior of the asymmetric AC-Ph-H/AC system was investigated at 2.0V. Fig. 9a shows that although the potential range in which the positive and negative electrodes operate during cell conditioning up to 2.0 V is different from that of the symmetrical AC/AC system, the values of the positive and negative electrodes remain within the stability window of both materials. This was confirmed by the negligible amount of gas evolved at the different cell voltages (Fig. 9c). Later, during the floating experiment at 2.0 V, the electrode potentials decrease after the first hours of floating and continue to stabilize at values lower than those of the symmetrical system (Fig. 9b). The complete absence of gas emission during the floating of the supercapacitor implies that in the asymmetric system both electrodes are operating within their stability potential window (Fig. 9d). Therefore, the combination of a positive electrode with a surface modification that protects against oxidation and lowers the pH_{PZC} to increase the oxidation potential, together with a negative electrode with a higher pH_{PZC} to decrease the reduction potential, is optimal.

Fig. 10a shows the capacitance retention during the floating test at 2.0 V cell voltage. A slight decrease in capacitance was observed during the first 10 h, from 100 to 90 F g^{-1}. Beyond this time, the capacitance remains quite stable up to 50 h of ageing, with capacitance retentions even higher than those of the symmetrical AC-Ph-H/AC-Ph-H supercapacitor. These results confirm that the asymmetric system is the right strategy to achieve cell voltages of 2.0 V, while for the symmetric system 1.8 V is the maximum voltage that leads to a correct ageing behavior (Fig. 2b).

Given the excellent ageing performance of the asymmetric system at 2.0 V, the cell voltage was increased to 2.2 V. Fig. 10a shows the capacitance retention during ageing at such a voltage. After a capacitance decrease from 130 to 90 F g^{-1} during the first 15 h, the capacitance value stabilizes at the same value as that obtained at 2.0 V. Therefore, even without optimizing the system in terms of electrode mass balance, it is clear that such an asymmetric configuration allows the system to operate at a cell voltage as high as 2.2 V.

At such a high cell voltage, the asymmetric system exhibits higher capacitances than the symmetric system at low current densities (Fig. 10b). However, the capacitance decreases to maintain the same value as the symmetric system when the current density is increased (Fig. 10c). In fact, Fig. 10c shows that after an initial decrease in capacitance when increasing the charge density, the asymmetric system presents an optimal charge capability.

Therefore, the asymmetric configuration combining a surface modified carbon with the raw material will allow to increase the stored energy and the power density compared to a symmetric configuration using the raw material.

In this sense, Fig. 10d presents the Ragone plot showing the energy and power densities for symmetric AC/AC and asymmetric AC/AC-Ph-H supercapacitors at the maximum cell voltage found during the ageing experiments (1.8 and 2.2 V, respectively). The maximum energy density and power density, defined here as the energy density extracted at 10 s discharge time, were improved by 2.1 and 4.5 times respectively for the asymmetric device. In particular, the maximum energy density that can be stored can be increased from 11.2 to 23.6 Wh kg^{-1} from the symmetric to the asymmetric system, while the energy density for 10 s discharge reaches 8.5 Wh kg^{-1} for the asymmetric system.

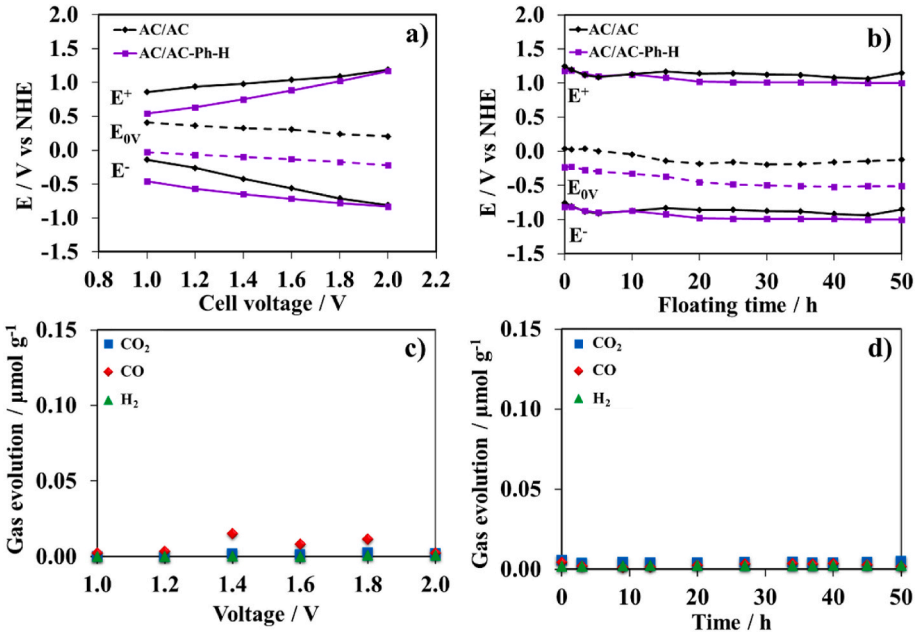

Fig. 9. Potential limits of positive (E^+) and negative (E^-) electrodes during conditioning the cell from 1.0 to 2.0 V (a) and during floating cell voltage at 2.0 V (b) of asymmetric and symmetric supercapacitors in 2 mol L^{-1} Li_2SO_4. The E_{0V} values (dashed lines) correspond to the electrodes potential when the working voltage is shifted to 0.0 V before each change of maximum voltage. Evolved gases amounts while polarization from 1.0 to 2.0 V (c) and as function of floating time at 2.0 V (d) of asymmetric supercapacitors built as AC/AC-Ph-H.

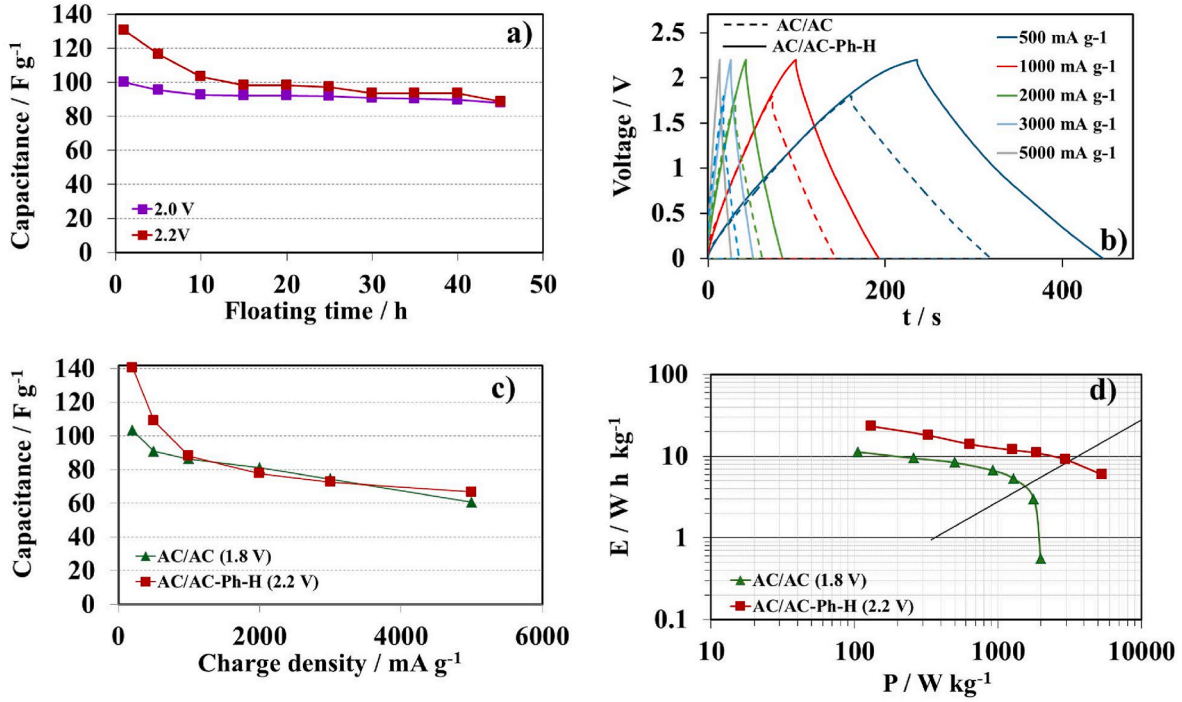

Fig. 10. Evolution of capacitance retention as a function of floating time of asymmetric AC/AC-Ph-H at 2.0 V and 2.2 V in 2 mol L^{-1} Li_2SO_4 (a). Comparison of electrochemical performance of AC/AC supercapacitor at 1.8 V of cell voltage and AC/AC-Ph-H supercapacitor at 2.2 V: galvanostatic charge/discharge at different charges densities (b), specific capacitance vs. charge density (c); Ragone plot related to energy and power densities (d). The line in the Ragone plot corresponds to 10 s discharge time.

4. Conclusions

The effect of the surface functionality of carbon-based electrodes in aqueous electrolytes has been investigated from the point of view of decreasing the carbon reactivity at the positive electrode to avoid electrode degradation and to increase the cell voltage. A detailed analysis was conducted by examining gas levels and compositions during ageing, alongside the evolution of the physicochemical properties of carbon electrodes and electrochemical performance.

The results show that the numerous active oxidation sites initially present on the carbon surface cannot be fully removed by thermal hydrogen treatment, which only saturates high-energy sites with unpaired electrons. Similarly, chemical oxidation offers limited protection to the positive electrode. In contrast, after a chemical grafting, the carbon show significantly higher oxidation resistance, as grafted groups block active sites at graphene layer edges. This protection is more effective when the phenyl group bonded to active sites lacks electron-withdrawing groups, like carboxylic acid. The combination of this active site blocking effect with a reduction in the pH_{PZC} to increase the oxidation potential is an effective strategy for protecting the positive electrode from oxidation, thereby increasing cell voltage and stored energy. An asymmetric system using the best-performing material (AC-Ph-H) as the positive electrode and unmodified carbon as the negative electrode enables long-term operation at a cell voltage up to 2.2V.

Therefore, protecting the surface of the positive electrode by grafting moieties that simultaneously lower the pH_{PZC} and block active sites for oxidation proves to be a valuable strategy. This approach increases the energy density by 2.1 times and the power density by 4.5 times in supercapacitors operating with aqueous electrolytes.

CRediT authorship contribution statement

Alicia Gomis Berenguer: Writing – review & editing, Writing – original draft, Validation, Methodology, Investigation, Conceptualization. **Martin Weissmann:** Methodology, Investigation, Formal analysis. **Rachelle Omnee:** Investigation, Formal analysis. **Encarnación Raymundo-Piñero:** Writing – review & editing, Writing – original draft, Visualization, Validation, Supervision, Project administration, Methodology, Funding acquisition, Conceptualization.

Declaration of competing interest

The authors declare the following financial interests/personal relationships which may be considered as potential competing interests: Alicia Gomis-Berenguer reports financial support was provided by European Union. Encarnacion Raymundo-Pinero reports financial support was provided by Centre-Val de Loire Region. If there are other authors, they declare that they have no known competing financial interests or personal relationships that could have appeared to influence the work reported in this paper.

Acknowledgements

ER-P, MW and RO thank the Région Centre Val de Loire (Project APR-IA PRESERVE convention nº 00134933; MATHYFON convention nº 240602) and RS2E for financial support. AG-B thanks European Union NextGenerationEU (ZAMBRANO21-10) for the funding.

References

[1] L. Demarconnay, E. Raymundo-Piñero, F. Béguin, A symmetric carbon/carbon supercapacitor operating at 1.6 V by using a neutral aqueous solution, Electrochem. Comm. 12 (2010) 1275–1278, https://doi.org/10.1016/j.elecom.2010.06.036.

[2] Q. Gao, L. Demarconnay, E. Raymundo-Piñero, F. Béguin, Exploring the large voltage range of carbon/carbon supercapacitors in aqueous lithium sulfate electrolyte, Energy Environ. Sci. 5 (2012) 9611–9617, https://doi.org/10.1039/C2EE22284A.

[3] K. Fic, G. Lota, M. Meller, E. Frackowiak, Novel insight into neutral medium as electrolyte for high-voltage supercapacitors, Energy Environ. Sci. 5 (2012) 5842–5850, https://doi.org/10.1039/C1EE02262H.

[4] N. Batisse, E. Raymundo-Piñero, Pulsed electrochemical mass spectrometry for operando tracking of interfacial processes in small-time-constant electrochemical

devices such as supercapacitors, ACS Appl. Mater. Interfaces 9 (2017) 41224–41232, https://doi.org/10.1021/acsami.7b12068.
[5] M. He, K. Fic, E. Frackowiak, P. Novák, E.J. Berg, Ageing phenomena in high-voltage aqueous supercapacitors investigated by in situ gas analysis, Energy Environ. Sci. 9 (2016) 623–633, https://doi.org/10.1039/C5EE02875B.
[6] M.P. Bichat, E. Raymundo-Piñero, F. Béguin, High voltage supercapacitor built with seaweed carbons in neutral aqueous electrolyte, Carbon 48 (2010) 4351–4361, https://doi.org/10.1016/j.carbon.2010.07.049.
[7] S.E. Chun, J.F. Whitacre, Investigating the role of electrolyte acidity on hydrogen uptake in mesoporous activated carbons, J. Power Sources 242 (2013) 137–140, https://doi.org/10.1016/j.jpowsour.2013.05.007.
[8] Q. Abbas, P. Ratajczak, P. Babuchowska, A.L. Comte, D. Bélanger, T. Brousse, F. Béguin, Strategies to improve the performance of carbon/carbon capacitors in salt aqueous electrolytes, J. Electrochem. Soc. 162 (2015) A5148–A5157, https://doi.org/10.1149/2.0241505jes.
[9] S.T. Vindt, E.M. Skou, The buffer effect in neutral electrolyte supercapacitors, Appl. Phys. A 122 (2016) 64, https://doi.org/10.1007/s00339-015-9563-8.
[10] Y. Yokoyama, T. Fukutsuka, K. Miyazaki, T. Abe, Origin of the electrochemical stability of aqueous concentrated electrolyte solutions, J. Electrochem. Soc. 165 (14) (2018) A3299–A3303, https://doi.org/10.1149/2.0491814jes.
[11] A. Slesinski, S. Sroka, K. Fic, E. Frackowiak, J. Menzel, Operando monitoring of local pH value changes at the carbon electrode surface in neutral sulfate-based aqueous electrochemical capacitors, ACS Appl. Mater. Interfaces 14 (33) (2022) 37782–37792, https://doi.org/10.1021/acsami.2c09920.
[12] P. Bujewska, P. Galek, K. Fic, Monitoring the ion population at a carbon electrode/aqueous electrolyte interface at various pHs using electrochemical dilatometry, Energy Storage Mater. 63 (2023) 103003, https://doi.org/10.1016/j.ensm.2023.103003.
[13] F. Béguin, K. Kierzek, M. Friebe, A. Jankowska, J. Machnikowski, K. Jurewicz, E. Fracowiak, Effect of various porous nanotextures on the reversible electrochemical sorption of hydrogen in activated carbons, Electrochim. Acta 51 (2006) 2161–2167, https://doi.org/10.1016/j.electacta.2005.03.086.
[14] L.R. Radovic, B. Bockrath, On the chemical nature of graphene edges: origin of stability and potential for magnetism in carbon materials, J. Am. Chem. Soc. 127 (2005), https://doi.org/10.1021/ja050124h, 5917-5127.
[15] T. Kyotani, J.-I. Ozaki, T. Ishii, What can we learn by analyzing the edge sites of carbon materials? Carbon Reports 1 (4) (2022) 188–205, https://doi.org/10.7209/carbon.010406.
[16] P. Azaïs, L. Duclaux, P. Florian, D. Massiot, M.A. Lillo-Ródenas, A. Linares-Solano, J.P. Peres, C. Jehoulet, F. Béguin, Causes of supercapacitors ageing in organic electrolyte, J. Power Sourc. 171 (2007) 1046–1053, https://doi.org/10.1016/j.jpowsour.2007.07.001.
[17] R. Tang, K. Taguchi, H. Nishihara, T. Ishii, E. Morallón, D. Cazorla-Amorós, T. Asada, N. Kobayashi, Y. Muramatsu, T. Kyotani, Insight into the origin of carbon corrosion in positive electrodes of supercapacitors, J. Mater. Chem. A 7 (2019) 7480–7488, https://doi.org/10.1039/C8TA11005K.
[18] Y. Kawabe, Y. Miyakoshi, R. Tang, T. Fukuma, H.o Nishihara, Y. Takahashi, Nanoscale characterization of the site-specific degradation of electric double-layer capacitor using scanning electrochemical cell microscopy, Electrochem. Sci. Adv. 2 (2022) e2100053, https://doi.org/10.1002/elsa.202100053.
[19] H. Nishihara, T. Simura, S. Kobayashi, K. Nomura, R. Berenguer, M. Ito, M. Uchimura, H. Iden, K. Arihara, A. Ohma, Y. Hayasaka, T. Kyotani, Oxidation-resistant and elastic mesoporous carbon with single-layer graphene walls, Adv. Funct. Mater. 26 (2016) 6418–6427, https://doi.org/10.1002/adfm.201602459.
[20] Y. Sato, N. Yamada, S. Kitano, D. Kowalski, Y. Aoki, H. Habazaki, High-corrosion-resistance mechanism of graphitized platelet-type carbon nanofibers in the OER in a concentrated alkaline electrolyte, J. Mater. Chem. A 10 (2022) 8208, https://doi.org/10.1039/d2ta00133k.
[21] G. Alemany-Molina, B. Martínez-Sánchez, E. Morallón, D. Cazorla-Amorós, The role of oxygen heteroatoms in the surface (electro)chemistry of carbon materials, Carbon Reports 1 (4) (2022) 162–174, https://doi.org/10.7209/carbon.010405.
[22] M. Antonietti, M. Oschatz, The concept of "Noble, heteroatom-doped carbons," Their directed synthesis by electronic band control of carbonization, and applications in catalysis and energy materials, Adv. Mater. 30 (2018) 1706836, https://doi.org/10.1002/adma.201706836.
[23] H.-F. Xia, B. Zhang, C.-H. Wang, L. Cao, B. Luo, X-m. Fan, J-f. Zhang, X. Ou, Surface engineered carbon-cloth with broadening voltage window for boosted energy density aqueous supercapacitors, Carbon 162 (2020) 136e146, https://doi.org/10.1016/j.carbon.2020.02.033.
[24] R. Berenguer, R. Ruiz-Rosas, A. Gallardo, D. Cazorla-Amoros, E. Morallon, H. Nishihara, T. Kyotani, J. Rodríguez-Mirasol, T. Cordero, Enhanced electro-oxidation resistance of carbon electrodes induced by phosphorus surface groups, Carbon 95 (2015) 681–689, https://doi.org/10.1016/j.carbon.2015.08.101.
[25] M. Yu, Z. Wang, H. Zhang, P. Zhang, T. Zhang, X. Lu, X. Feng, Amino functionalization optimizes potential distribution: a facile pathway towards high-energy carbon-based aqueous supercapacitors, Nano Energy 65 (2019) 103987.
[26] A. Slesinski, C. Matei-Ghimbeu, K. Fic, F. Beguin, E. Frackowiak, Self-buffered pH at carbon surfaces in aqueous supercapacitors, Carbon 129 (2018) 758e765, https://doi.org/10.1016/j.carbon.2017.12.101.
[27] R. Ruiz-Rosas, I. Fuentes, C. Viñas, F. Teixidor, E. Morallon, D. Cazorla-Amoros, Tailored metallacarboranes as mediators for boosting the stability of carbon-based aqueous supercapacitors, Sustain. Energy Fuels 2 (2018) 345, https://doi.org/10.1039/c7se00503b.
[28] B. Desalegn Assresahegn, T. Brousse, D. Bélanger, Advances on the use of diazonium chemistry for functionalization of materials used in energy storage systems, Carbon 92 (2015) 362–381, https://doi.org/10.1016/j.carbon.2015.05.030.
[29] M. Amiri, G. Shul, N. Donzel, D. Bélanger, Aqueous electrochemical energy storage system based on phenanthroline- and anthraquinone-modified carbon electrodes, Electrochim. Acta 390 (2021) 138862, https://doi.org/10.1016/j.electacta.2021.138862.
[30] T. Menanteau, C. Benoît, T. Breton, C. Cougnon, Enhancing the performance of a diazonium-modified carbon supercapacitor by controlling the grafting process, Electrochem. Commun. 63 (2016) 70–73, https://doi.org/10.1016/j.elecom.2015.12.014.
[31] G. Pognon, T. Brousse, D. Bélanger, Effect of molecular grafting on the pore size distribution and the double layer capacitance of activated carbon for electrochemical double layer capacitors, Carbon 49 (2011) 1340–1348, https://doi.org/10.1016/j.carbon.2010.11.055.
[32] T.J. Bandosz, C.O. Ania, Surface chemistry of activated carbons and its characterization, in: T.J. Bandosz (Ed.), Activated Carbon Surfaces in Environmental Remediation, Academic Press, New York, 2016, pp. 159–229.
[33] C.A. León y León, L.R. Radovic, Chemistry and physics of carbon, in: P.A. Thrower (Ed.) vol 24, Dekker, New York, 1994.
[34] J.A. Menéndez, J. Phillips, B. Xia, L.R. Radovic, On the modification and characterization of chemical surface properties of activated carbon: Microcalorimetric, electrochemical, and thermal desorption probes, Langmuir 13 (1997), https://doi.org/10.1021/la9602022, 3414-3412.